



Universiteit
Leiden
The Netherlands

Stimulating the autophagic-lysosomal axis enhances host defense against fungal infection in a zebrafish model of invasive Aspergillosis

Forn Cuni, G.; Welvaarts, L.; Stel, F.M.; Hondel, C.A.M.J.J. van den; Arentshorst, M.; Ram, A.F.J.; Meijer, A.H.

Citation

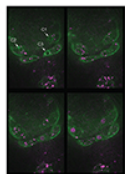
Forn Cuni, G., Welvaarts, L., Stel, F. M., Hondel, C. A. M. J. J. van den, Arentshorst, M., Ram, A. F. J., & Meijer, A. H. (2022). Stimulating the autophagic-lysosomal axis enhances host defense against fungal infection in a zebrafish model of invasive Aspergillosis. *Autophagy*, 1-14.
doi:10.1080/15548627.2022.2090727

Version: Publisher's Version

License: [Creative Commons CC BY-NC-ND 4.0 license](https://creativecommons.org/licenses/by-nc-nd/4.0/)

Downloaded from: <https://hdl.handle.net/1887/3436064>

Note: To cite this publication please use the final published version (if applicable).



Autophagy



ISSN: (Print) (Online) Journal homepage: <https://www.tandfonline.com/loi/kaup20>

Stimulating the autophagic-lysosomal axis enhances host defense against fungal infection in a zebrafish model of invasive Aspergillosis

G Forn-Cuní, L Welvaarts, FM Stel, CJ van den Hondel, M Arentshorst, AFJ Ram & AH Meijer

To cite this article: G Forn-Cuní, L Welvaarts, FM Stel, CJ van den Hondel, M Arentshorst, AFJ Ram & AH Meijer (2022): Stimulating the autophagic-lysosomal axis enhances host defense against fungal infection in a zebrafish model of invasive Aspergillosis, *Autophagy*, DOI: [10.1080/15548627.2022.2090727](https://doi.org/10.1080/15548627.2022.2090727)

To link to this article: <https://doi.org/10.1080/15548627.2022.2090727>



© 2022 The Author(s). Published by Informa UK Limited, trading as Taylor & Francis Group.



[View supplementary material](#)



Published online: 01 Jul 2022.



[Submit your article to this journal](#)



Article views: 486



[View related articles](#)



[View Crossmark data](#)

RESEARCH PAPER

 OPEN ACCESS 

Stimulating the autophagic-lysosomal axis enhances host defense against fungal infection in a zebrafish model of invasive Aspergillosis

G Forn-Cuní , L Welvaarts , FM Stel , CJ van den Hondel , M Arentshorst , AFJ Ram , and AH Meijer 

Institute of Biology Leiden, Leiden University, Leiden, The Netherlands

ABSTRACT

The increasing prevalence of antifungal-resistant human pathogenic fungi, particularly azole-resistant *Aspergillus fumigatus*, is a life-threatening challenge to the immunocompromised population. Autophagy-related processes such as LC3-associated phagocytosis have been shown to be activated in the host response against fungal infection, but their overall effect on host resistance remains uncertain. To analyze the relevance of these processes *in vivo*, we used a zebrafish animal model of invasive Aspergillosis. To confirm the validity of this model to test potential treatments for this disease, we confirmed that immunosuppressive treatments or neutropenia rendered zebrafish embryos more susceptible to *A. fumigatus*. We used GFP-Lc3 transgenic zebrafish to visualize the autophagy-related processes in innate immune phagocytes shortly after phagocytosis of *A. fumigatus* conidia, and found that both wild-type and melanin-deficient conidia elicited Lc3 recruitment. In macrophages, we observed GFP-Lc3 accumulation in puncta after phagocytosis, as well as short, rapid events of GFP-Lc3 decoration of single and multiple conidia-containing vesicles, while neutrophils covered single conidia-containing vesicles with bright and long-lasting GFP-Lc3 signal. Next, using genetic and pharmacological stimulation of three independent autophagy-inducing pathways, we showed that the antifungal autophagy response improves the host survival against *A. fumigatus* infection, but only in the presence of phagocytes. Therefore, we provide proof-of-concept that stimulating the (auto)phagolysosomal pathways is a promising approach to develop host-directed therapies against invasive Aspergillosis, and should be explored further either as adjunctive or stand-alone therapy for drug-resistant *Aspergillus* infections.

ARTICLE HISTORY

Received 9 September 2021
Revised 8 June 2022
Accepted 13 June 2022

KEYWORDS

Aspergillus; autophagic defense; fungal infection; host-pathogen interaction; immunomodulation; innate immunity; phagocytes; zebrafish



Introduction


Air can contain thousands to billions of fungal spores per cubic meter [1]. Although easily neutralized by a competent immune system, spores from pathogenic fungal species germinate inside immunocompromised hosts, causing life-threatening conditions that result in over 1.6 million deaths annually [2]. Saprophytic fungi of the genus *Aspergillus* cause invasive Aspergillosis (IA), one of the most common serious clinical mycoses. Current antibiotic treatment options against IA are limited – amphotericin B, medical triazoles, and echinocandins – and, even when treated, IA has 50% to 90% mortality rate in certain populations [3–5]. Alarming, triazole-resistant *Aspergillus fumigatus* strains are becoming more common in treatment-naïve patients [6] while the population at risk of contracting IA increases due to comorbidity with other infectious diseases like AIDS, influenza, and tuberculosis; leukemia; and the widespread use of immunosuppressive treatments against transplant rejections and autoimmune diseases [7–10]. Therefore, new treatments for IA are desperately required.

Host-directed therapies (HDTs) aim to empower the host to effectively fight an infection instead of directly targeting the pathogen and have been proposed as an adjunctive treatment for infections caused by antibiotic-resistant microbes, including fungi [11–13]. A promising target for HDT development

against IA is the autophagy-lysosomal degradative axis, together with its associated pathways [14–16]. In immunocompromised patients, circulating monocytes and tissue-resident immune cells, as alveolar macrophages in the lungs, are the first – and sometimes only – line of defense against fungal invasions [17]. These professional phagocytes detect specific conserved pathogen associated molecular patterns (PAMPs) in the fungal cell wall through their pattern recognition receptors (PRRs) [18], upon which they internalize the conidia and coordinate the host antifungal response [19]. Once internalized, conidia-containing vesicles may be targeted by autophagy-related mechanisms to be degraded by ultimately fusing them with lysosomes [20,21].

Autophagy-related mechanisms include selective autophagy and LC3-associated phagocytosis (LAP), both identified as powerful defense mechanisms activated downstream of spore recognition in innate immune phagocytes during fungal invasions [22–24]. However, DHN-melanin, a principal component of the *A. fumigatus* conidial cell-wall, impairs autophagy in macrophages and the subsequent oxidative burst meant to kill the germinating spores, presumably via intracellular calcium sequestration [24,25]. Thus, lack of activation of the host autophagy machinery could be a limiting factor during *A. fumigatus* infections, and therefore increasing autophagic activity is a potential therapeutic strategy for treating IA.

CONTACT G Forn-Cuní Institute of Biology Leiden, Leiden University, Einsteinweg 55, Leiden, The Netherlands  g.forn-cuni@biology.leidenuniv.nl; AH Meijer Institute of Biology Leiden, Leiden University, Einsteinweg 55, 2333CC Leiden, The Netherlands  a.h.meijer@biology.leidenuniv.nl

 Supplemental data for this article can be accessed online at <https://doi.org/10.1080/15548627.2022.2090727>

© 2022 The Author(s). Published by Informa UK Limited, trading as Taylor & Francis Group.

This is an Open Access article distributed under the terms of the Creative Commons Attribution-NonCommercial-NoDerivatives License (<http://creativecommons.org/licenses/by-nc-nd/4.0/>), which permits non-commercial re-use, distribution, and reproduction in any medium, provided the original work is properly cited, and is not altered, transformed, or built upon in any way.

To test the possible effect of autophagy-enhancing drugs against *A. fumigatus* *in vivo*, we used a previously characterized model of IA in zebrafish embryos [26,27]. The infection of *A. fumigatus* conidia in the hindbrain of 36 h post fertilization (hpf) zebrafish embryos recreates the multicellular environment and dynamics of clinical infections and has already provided insights into the host-pathogen interaction of this human disease [27–29]. Using zebrafish embryos as preclinical animal model has several benefits for the objective of this study: they have demonstrated translational impact, are optically transparent, genetically tractable, suitable for drug discovery, well-established for antimicrobial autophagy research, and – of special relevance to this field – do not possess active adaptive immunity during the experiments [27,30–32], rendering them susceptible to *Aspergillus* infections and effectively mimicking the immunocompromised population at risk of developing this disease.

Here, we confirm that the zebrafish embryo infection model recreates the major susceptibilities of human clinical IA, describe the autophagy activation dynamics of innate immunity phagocytes after wild-type and DHN-melanin-deficient *A. fumigatus* conidial phagocytosis, and reveal the differential Lc3 recruitment to conidia-containing vesicles in macrophages and neutrophils. We also report how both genetic and chemical stimulation of (auto)phagolysosomal pathways improves the host defense outcome against *A. fumigatus* infection *in vivo*.

Results

The zebrafish embryo – *A. fumigatus* hindbrain infection model recapitulates clinically-relevant phenotypes of IA

Previous research has unraveled mechanisms of the pathogenesis and the host-pathogen interaction of *A. fumigatus* infections using the zebrafish hindbrain infection model (Figure 1 (a)), which included the recapitulation of clinical phenotypes [26–29,33]. Therefore, in order to test if this model would be suitable for drug discovery research, we first confirmed that this model reproduced the increased susceptibility phenotype under these conditions in our experimental setup.

The major reported risk factor for clinical IA is immunodeficiency, including prolonged therapy with immunosuppressants, neutropenia, and Chronic Granulomatous Disease [3]. To mimic the prolonged use of immunosuppressants, we treated zebrafish embryos with chronic, non-developmentally toxic doses of cyclosporin A, tacrolimus (FK506), and rapamycin – acting on immunophilins – and the glucocorticoid dexamethasone. Except for tacrolimus, for which we found no effect on the mortality at nontoxic doses, all immunosuppressive treatments diminished embryo survival against *A. fumigatus* infection compared to the infected embryos treated with vehicle dimethyl sulfoxide (DMSO) (Figure 1(b, e)). To model chronic granulomatous disease, we generated F0 *cyba* (cytochrome b-245, alpha polypeptide) loss-of-function mutants in zebrafish embryos using CRISPR-Cas9 as recently described [34], as well as used a previously characterized morpholino against *cyba/p22^{phox}* to transiently knock down *Cyba* for the duration of the experiment [33].

In concordance with infections with *A. nidulans*, knocking out this NADPH oxidase subunit in zebrafish embryos also led to significantly increased mortality during *A. fumigatus* infection (Figure 1(f), Figure S1A). We then simulated neutropenia by chemically depleting neutrophils using a transgenic line expressing the bacterial nitroreductase (NTR) under a neutrophil-specific promoter. NTR catalyzes the reduction of the innocuous prodrug metronidazole (MTZ), thereby producing a cytotoxic product that induces cell death specifically in neutrophils [35]. The depletion of neutrophils after MTZ treatment was confirmed via stereo imaging of the fluorescently labeled neutrophils. Consistent with clinical data, neutropenic fish were more susceptible to the fungal infection, while MTZ did not have a significant effect on the infection in non-transgenic zebrafish (Figure 1(g), Figure S1B).

In all, the hindbrain infection of 36 hpf zebrafish embryos with *A. fumigatus* conidia recapitulates the clinically reported increased IA susceptibility during immunodeficiency treatment in our experimental setup, supporting its relevance as an *in vivo* model to study drug effects and host defense in this disease.

Phagocytes activate autophagy-related processes to degrade *A. fumigatus* conidia *in vivo*.

To rationally devise effective host-directed strategies, we focused on the interaction between innate immune cells and phagocytosed *A. fumigatus* conidia, looking for limitations that allow *Aspergillus* to thrive intracellularly. *In vivo* imaging in the zebrafish *A. fumigatus* infection model allowed us to evaluate the consequence of differences in timing and arrival of innate immune cells to the infection foci. We found that these differences resulted in a range of dynamic and heterogeneous responses in each infection. For example, while most macrophages phagocytose a similar amount of conidia *in vitro*, in an *in vivo* setting some phagocytes arrive early at the infection foci and phagocytose most of the spores while others only phagocytose a minimal number of conidia (Figure 2(a), Movie S1). Phagocytes in the zebrafish hindbrain then aggregate over the next 24 h, forming granuloma-like structures from within conidia eventually germinate [28,36]. We reasoned that in those instances intracellular pathways for fungal degradation would be overburdened with the high amount of cargo to be degraded, which prompted us to investigate the response of the autophagy machinery.

It has recently been reported that microbial-targeted autophagy (xenophagy) and its related process LAP contribute to efficient intracellular fungal clearance by innate immune cells *in vitro* [22–24]. To visualize the *in vivo* autophagy activation dynamics in innate immune cells after *A. fumigatus* phagocytosis, we imaged the fluorescent *map1lc3b/Lc3b* reporter zebrafish line Tg(CMV:EGFP-*map1lc3b*)^{zf155} [37] or Tg(*bactin:mCherry-map1lc3b*) [38] – further referred to as GFP-Lc3 and mCherry-Lc3, respectively – by confocal microscopy shortly after infection. These transgenic lines allow the study of autophagy-related dynamics in real time by analyzing the accumulation of fluorescently labeled Lc3b in specific vesicles (Figure 2, Movie S2). Focusing on immune cells shortly after

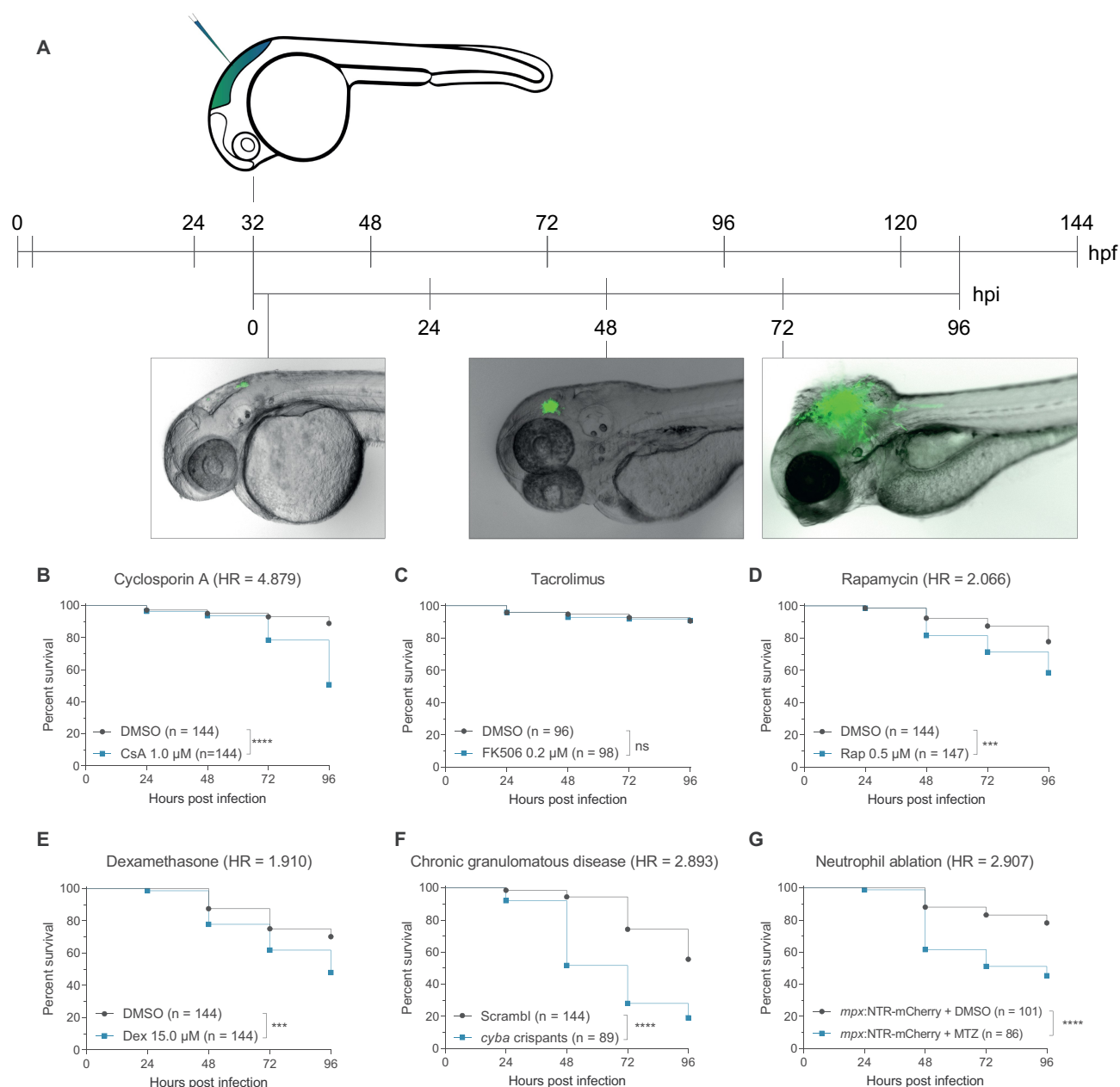


Figure 1. The zebrafish embryo model recapitulates susceptibilities of clinical IA. (a) Schematic representation of the zebrafish embryo – *A. fumigatus* infection model. Conidia of *A. fumigatus* D141 expressing an EGFP fluorescent plasmid were injected in the hindbrain at 32 hpf and representative images of infection at 2, 48 and 72 h post infection are shown. (b, c, d, and e) Survival curves of zebrafish embryos infected with *A. fumigatus* Δ Ku80 and exposed via waterborne treatment to 1 μ M of cyclosporin A (b), 0.2 μ M of FK506 (c), 0.5 μ M of rapamycin (d), 15 μ M of dexamethasone (e), or DMSO as a vehicle control at the same v/v. (f) Survival curves of *cyba* crispants or *scramble* control zebrafish embryos infected with *A. fumigatus* Δ Ku80. (g) Survival curves of zebrafish embryos with or without neutrophil ablation with metronidazole infected with *A. fumigatus* Δ Ku80. (b, d and f) are representative of at least 3 independent biological replicates, while (c) is representative of 2 independent biological replicates. The hazard ratio (HR) indicated is calculated vs. the control condition using the logrank method. Significance in the curve comparison is calculated using Log-rank (Mantel-Cox test): ns non-significant; * $P \leq 0.05$; ** $P \leq 0.01$; *** $P \leq 0.001$; **** $P \leq 0.0001$.

phagocytosis, we observed dynamic autophagy-related processes, including transient GFP-Lc3 accumulation in small vesicles (“Lc3 puncta”) (Figure 2(d,e)) or covering the whole conidia-containing vesicle (“Lc3 rings”), which sometimes contained individual conidia or consisted of larger compartments with multiple conidia (Figure 2(c,f,g)). These processes were active during at least the first 24 h post infection, where

some conidia already started to germinate and the hyphal structure was surrounded by GFP-Lc3 (Figure 2(h,i)). However, probably affected by the high amount of variability explained above, we could not detect a consistent activation pattern of these processes after phagocytosis.

Thus, our *in vivo* results revealed that phagocytes actively engage conidia with autophagy-related processes directed

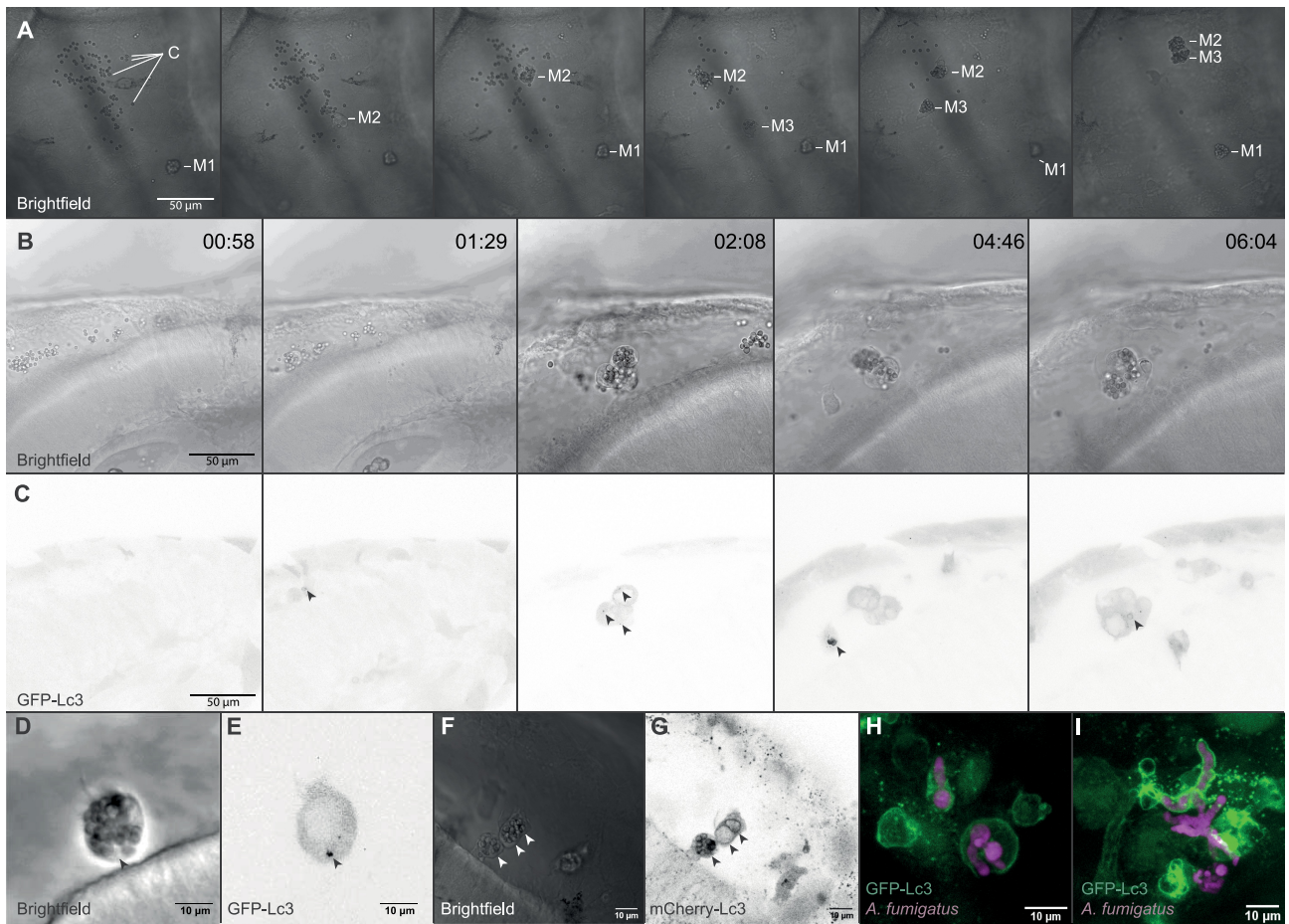


Figure 2. GFP-Lc3 dynamics in phagocytes after phagocytosing *A. fumigatus* conidia. (a) Representative sequence of events following injection of *A. fumigatus* conidia into the hindbrain of a zebrafish embryo. More than 100 *A. fumigatus* $\Delta Ku80$ conidia are initially phagocytosed by the first 3 macrophages to arrive at the infection foci. Arrows indicate macrophage arrival and phagocytosis start. Images taken from Movie S1. (b and c) Confocal microscopy images showing the brightfield (b) or GFP-Lc3 fluorescence intensity (c) during the first 6 h and 30 min after infection. Most conidia are phagocytosed in the first 5 h post infection by a small number of phagocytes. Arrows indicate GFP-Lc3 levels in immune cells after phagocytosing *A. fumigatus* conidia, including individual GFP-Lc3 rings around the conidia. Images taken from Movie S2. (d and e) Brightfield (d) and GFP-Lc3 fluorescence intensity (e) of a macrophage with several conidia showing a GFP-Lc3 puncta. (f and g) Brightfield (f) and mCherry-Lc3 fluorescence intensity (g) confocal microscopy images showing mCherry-Lc3 accumulation across vesicles with individual and multiple spores. (h and i) Confocal images of GFP-Lc3 accumulation around germinating conidia of *A. fumigatus* D141 expressing dsRed fluorescent plasmid [40] in the hindbrain of zebrafish embryos fixed 15 h post infection.

toward degrading *A. fumigatus* conidia and hyphae during the first hours after infection, but these processes are not enough to stop fungal germination during acute infection.

Differential autophagy dynamics between macrophages and neutrophils

Circulating macrophages are the main responders to *A. fumigatus* infection in the zebrafish hindbrain, and neutrophils are mostly engaged in a later stage [36,39,40]. This behavior effectively simulates the phagocyte recruitment dynamics reported in the lungs of human patients and IA mice models, in which alveolar macrophages are already present at the infection site while polymorphonuclear neutrophils migrate to the infection focus and engage in killing hyphae [17,41]. However, despite efficiently phagocytosing *A. fumigatus* conidia and restricting their rapid extracellular growth, it has been shown that macrophages are unable to kill

the fungal spores and create a replication niche from within the infection can be established [28].

To study the differential autophagy dynamics in macrophages and neutrophils, we combined the GFP-Lc3 zebrafish line with a macrophage marker Tg(CMV:*map1lc3b*-EGFP^{zf155}; *mpeg1.1*:mCherry^{F^{ump2}}) and analyzed the GFP-Lc3 colocalization with conidia in the first hours post infection. Confirming previous results, most conidia were phagocytosed by *mpeg1.1*-positive phagocytes – that is, macrophages (Figure 3(a,b)). However, non-labeled phagocytes also phagocytosed a smaller number of conidia (Figure 3(a,b,f)). We refer to these phagocytes as neutrophils since zebrafish embryos do not contain other innate immune phagocytes than macrophages and neutrophils at this developmental stage [42]. In the rare events of conidial phagocytosis by neutrophils, we observed strong GFP-Lc3 rings targeting single conidia (Figure 3(d-f), Movie S3), while in macrophages we saw small GFP-Lc3 puncta, and weaker transient GFP-Lc3 rings targeting vesicles which usually contained multiple

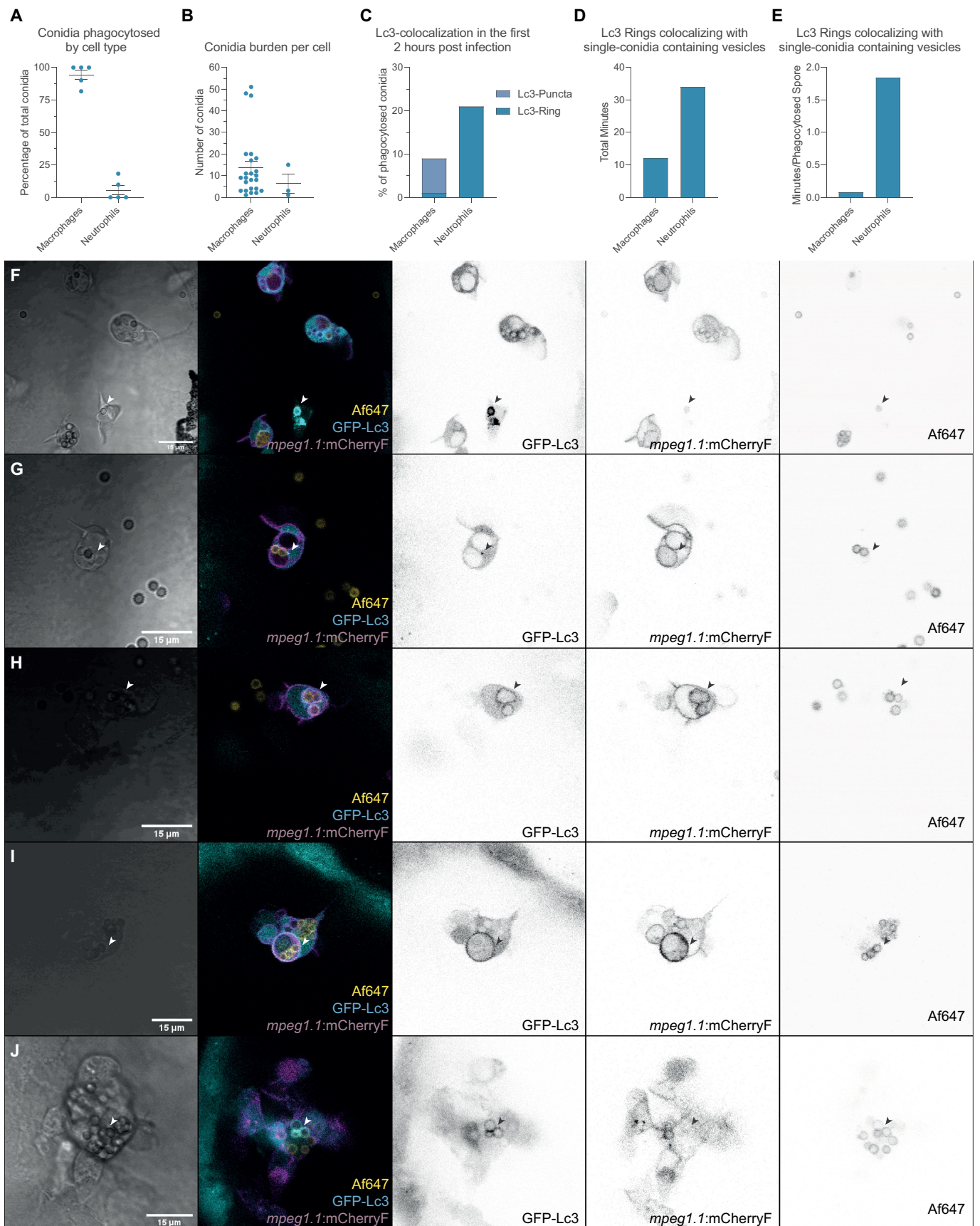


Figure 3. Differential GFP-Lc3 dynamics in phagocytes after phagocytosing *A. fumigatus* conidia. (a, b, c, d, and e) Quantification of phagocytosis and Lc3 dynamics in 15 hours of timelapse imaging from 5 individual larvae infected with *A. fumigatus* Δ Ku80 conidia during the first hours post infection. (a) Most of the injected conidia in the zebrafish hindbrain are phagocytosed by macrophages, and (b) macrophages phagocytose more conidia per cell than neutrophils. (c, d, and e) In the events of conidial phagocytosis by neutrophils, we observed rapid bright Lc3 rings covering single-conidia vesicles, while Lc3 decoration of conidia-containing vesicles in macrophages was scarcer in the first hours post infection. (f) A non-labeled phagocyte (neutrophil, N) strongly mobilizes GFP-Lc3 to single conidia-

conidia and continued after forming cellular aggregates (Figure 3(g–j)).

Thus, we show GFP-Lc3 recruitment by macrophages and neutrophils in response to *A. fumigatus* phagocytosis. Phagocytosis of conidia by neutrophils was rare, but neutrophils were able to efficiently mobilize GFP-Lc3 into vesicles containing single conidia, while macrophages efficiently phagocytosed most conidia and showed GFP-Lc3 responses.

Suppression of autophagy pathways increases susceptibility to *A. fumigatus* infection

To examine the relevance of the autophagy responses that we observed on the overall host defense against *A. fumigatus*, we studied the survival of zebrafish embryos after specific suppression of either LAP or selective autophagy. To do so, we knocked down either *rubcn*/*Rubcn* (rubicon autophagy regulator) – the master regulator of LAP – using a previously characterized morpholino [43], or *atg13*/*Atg13* (autophagy related 13 homolog (*S. cerevisiae*)) – required for autophagy initiation but not LAP – via biallelic F0 loss-of-function mutants as well as a previously validated morpholino [44]. Both treatments increased the susceptibility to *A. fumigatus* infection (Figure 4(a,b), Figure S1C). Contrasting, mutants of the classical intracellular autophagy receptor *sqstm1*/p62 (sequestosome 1), did not show increased mortality due to infection (Figure 4(c)). These results suggest that different autophagy-related processes, including LAP and *Sqstm1*-independent autophagy, are involved in host defense against *A. fumigatus*.

It has also been reported how the *A. Fumigatus* DHN-melanin layer can impair autophagy activation and the subsequently conidial degradation in macrophages [24,25,45]. In concordance, Δ *pksP* mutant conidia, which lack the DHN-melanin conidial layer, are highly targeted by autophagy processes and subsequently degraded in macrophages *in vitro*. We therefore tested the potential difference in virulence between DHN-melanin-deficient and wild-type *A. fumigatus* in our model. We confirmed that, as reported in mammals, Δ *pksP* caused less mortality at the same infection load (Figure 4(d)). In addition, the requirement of both *Rubcn*- and *Atg13*-related autophagy processes to protect against the infection was more evident with the melanin-deficient Δ *pksP* spores than with the wild-type spores (Figure 4(e,f), Figure S1D). This suggests that autophagy processes are more effective in fungal defense in the absence of DHN-melanin *in vivo*.

Given the improved defense against Δ *pksP* conidia and the higher susceptibility after autophagy-related knockdowns, we investigated a possible differential involvement of autophagy processes in the defense against wild-type and mutant conidia. Previous research has shown how MTOR (mechanistic target of rapamycin kinase) and LC3 preferentially colocalize with

Δ *pksP* compared to wild-type vesicles in macrophages *in vitro* [46]. Similar as described above for infections with wild-type spores, most of the Δ *pksP* conidia were phagocytosed by macrophages, but we observed several cases of strong and long-lasting GFP-Lc3-targeting of single conidia vesicles in neutrophils (Figure 4(g–m)). Contrasting, macrophages commonly targeted conidia with GFP-Lc3 in transient bursts shortly after phagocytosis, except for a rare case of intense GFP-Lc3 decoration in a macrophage (Figure 4(n), Movie S4). However, in this last case, the macrophage had also phagocytosed swollen conidia, thus probably having a higher exposure to fungal pathogen associated molecular patterns.

Overall, suppression of autophagy-related pathways in the host by *Atg13* or *Rubcn* loss of function results in a higher infection-related mortality. The increased susceptibility of autophagy impaired zebrafish hosts was observed in infections with wild type conidia and became more pronounced in infections with melanin-deficient conidia. We noticed an increase in the single-conidia targeting of macrophages in melanin-deficient conidia in contrast to wild-type spores, but were not able to detect significantly different GFP-Lc3 targeting dynamics. In both cases, the strongest GFP-Lc3 responses were observed in neutrophils, not in macrophages. These results are consistent with our hypothesis that suboptimal activation of the host autophagy machinery in macrophages is a limiting factor during IA *in vivo*, and therefore a potential druggable target to treat IA.

Stimulating the (auto)phagolysosomal axis increases the host survival against IA

Given the correlation between autophagy activation and host survival both in wild-type and Δ *pksP* conidia infections, we asked if stimulating these autophagy-related processes can tip the balance in favor of lysosomal degradation, thus improving the host defense against *A. fumigatus* *in vivo*.

To do so, we infected zebrafish embryos with wild type *A. fumigatus* and treated them with chemical autophagy activators acting through different mechanisms, including AR-12 (Mtor-independent autophagy induction via *Pdk1* inhibition and endoplasmic reticulum stress), torin-1 (autophagy induction via interaction with Mtor), and carbamazepine (Mtor-independent induction of autophagy via the inositol pathway). All autophagy-inducing treatments consistently increased host survival during *A. fumigatus* infection in comparison to their DMSO control, regardless of their mode of action (Figures 5(a–c)). To rule out a direct antifungal effect, we added the chemicals directly to *A. fumigatus* culture and found no effect on growth or germination at the concentrations tested (Figure S2).

In addition to the drug treatment, we used a genetic strategy to enhance autophagy. We previously characterized *dram1*/*Dram1* (DNA-damage regulated autophagy

containing vesicles shortly after phagocytosis (arrowheads), while labeled mCherryF-macrophages show high GFP-Lc3 fluorescence but not colocalizing with *A. fumigatus* Δ *Ku80* conidia labeled with Alexa Fluor™ NHS 647 (Af647). Image taken from the Movie S3. (G, H, I, and J) Examples of GFP-Lc3 puncta (g), and GFP-Lc3 signal around single (h) or multiple conidia (h and i) in mCherryF labeled macrophages. Note that the membrane-bound mCherryF signal of macrophages colocalizes with GFP-Lc3 signal after conidia phagocytosis. Contrasting to the bright GFP-Lc3 signal in neutrophils (f), macrophages show weaker GFP-Lc3 targeting to phagocytosed conidia. (j) GFP-Lc3 targeting of single-conidia continues during the first hours after formation of a granuloma-like structure.

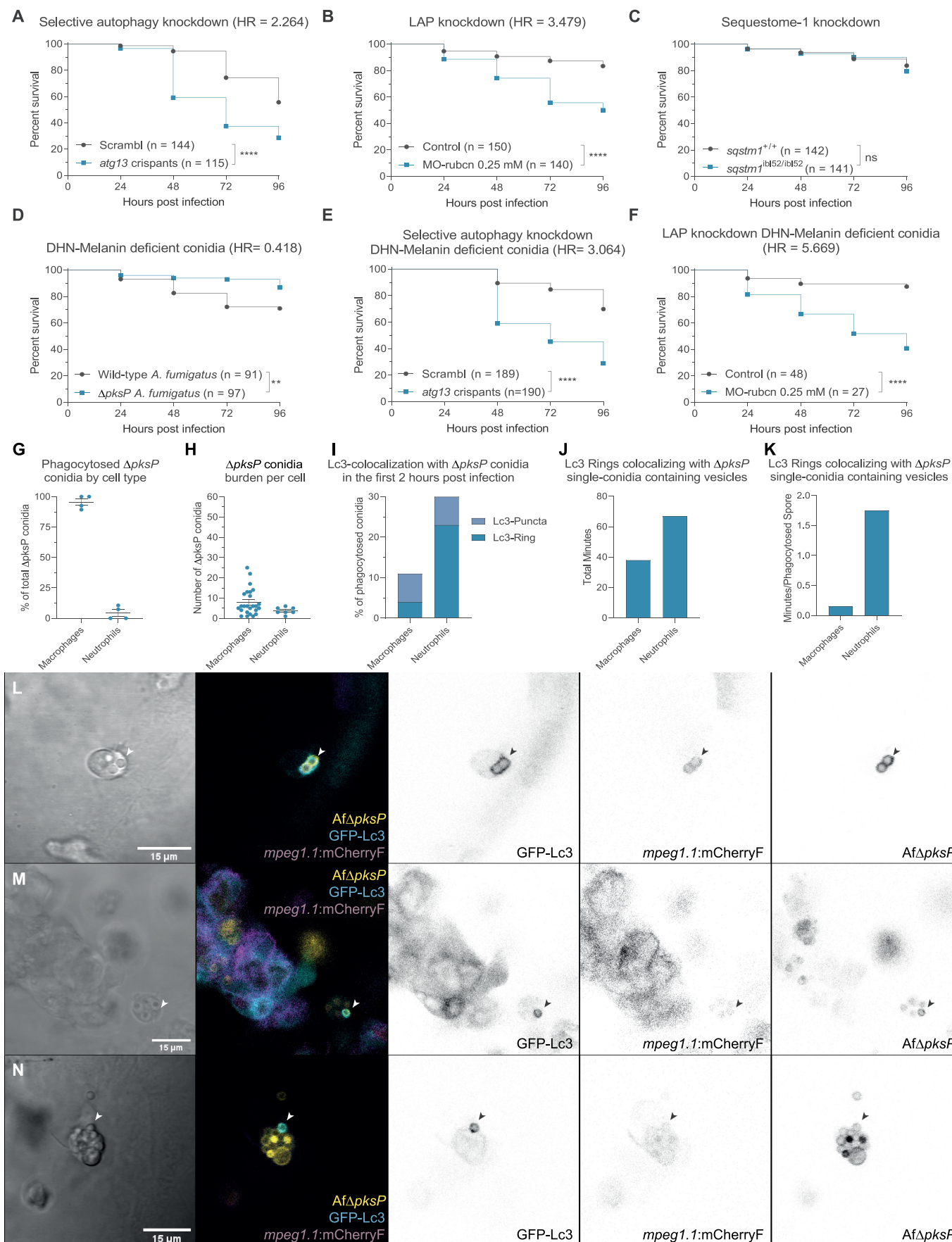


Figure 4. Suppression of autophagy pathways increases susceptibility to *A. fumigatus* infection. (a and b) Survival curves of *atg13* mutation (a) or *rubcn* (b) knockdown or control zebrafish embryos infected with *A. fumigatus* $\Delta Ku80$. (c) Survival curve of *sqstm1* mutants or non-mutant siblings infected with *A. fumigatus* $\Delta Ku80$. (d) Survival curve of zebrafish embryos infected with equal inoculum (150 conidia) of *A. fumigatus* $\Delta Ku80$ or DHN-Melanin-deficient *A. fumigatus* $\Delta pksP$. (e) and

modulator 1) as an enhancer of (auto)phagosome-lysosome fusion that is effective in host defense against infections of intracellular bacterial pathogens, including *Mycobacterium* and *Salmonella* [47,48]. While, similarly to *sqstm1*, *dram1* was not a requirement for efficient fungal defense (Figure 5(d)), its overexpression led to a significantly improved infection outcome (Figure 5(e)).

Given that all treatments performed affected the whole individual and not only immune cells, we wanted to gain additional insights in the effect and importance of these processes specifically in phagocytes dealing with *A. fumigatus* conidia. To do so, we knocked down *spi1b*/Spi1b (Spi-1 proto-oncogene b) in zebrafish embryos, which inhibits de-differentiation of immune cells into macrophages and neutrophils in zebrafish larvae during the duration of these experiments [49]. As expected, zebrafish larvae without innate immune cells were extremely susceptible to *A. fumigatus* infection (Figure S1E). In these cases, treatment with autophagy-inducing drugs did not increase the survival of zebrafish embryos to the infection (Figure 5(f)), confirming that phagocytes are required for the beneficial effect of inducing autophagy, and that these drugs are not affecting the virulence of *A. fumigatus* in zebrafish embryos. Therefore, we conclude that these autophagy-inducing drugs increase the survival to *A. fumigatus* infection in a host immune-dependent manner and do not affect the growth or virulence of *A. fumigatus*.

Finally, using an mCherry-Dram1 construct [38], we demonstrated that Dram1 colocalizes with *A. fumigatus* conidia in phagocytes (Figure 5(g)), supporting the conclusion that this autophagy-stimulating factor contributes to the response of phagocytes to *A. fumigatus*.

In all, we demonstrate that activating the (auto)phagolysosomal axis via either chemical or genetic means increases resistance against *A. fumigatus* infection in a host-dependent manner *in vivo*.

Discussion

Infections caused by azole-resistant *Aspergillus* pose a life-threatening challenge to the immunocompromised population [50]. The ubiquitous use of azoles, not only for human therapy but also for food production and environment preservation, is driving a worldwide rise of antifungal resistance to this class of drugs, rendering current first-line clinical treatment options ineffective [6,51]. There is therefore an increasing need to diversify our antifungal treatments [17]. In addition to the discovery and application of new and improved

antifungals, HDTs offer a potential solution as adjunctive or standalone treatment to drug-resistant infections.

As exemplified here, the zebrafish embryo IA model provides a useful platform to study both the host-pathogen interaction in detail using intravital microscopy and to preclinically test the effect of drugs on a population level. We observed a high degree of variability in the immune response between infections, even with similar number of phagocytes in the infection foci and comparable infection loads. We believe that this heterogeneity (both in the host and the fungal cells) creates stochastic environments that lead to a dynamic relationship between host and pathogen, which mimics the individual variation seen in human disease and is therefore complementary to *in vitro* studies using homogeneous cell types. Despite this variability between individuals, population-level results, such as the increased susceptibility after treatment with corticosteroids as dexamethasone, are consistent with previous reports both in zebrafish and in humans, showing the robustness of the model for drug discovery [28,52]. A notable exception was the treatment with the Ppp3/calcein inhibitor FK506, in which we could not reproduce a higher susceptibility at concentrations that did not affect the normal embryo development [29,53]. These differences may be due to fungal or zebrafish strains used, which are known to affect infection dynamics [26,40,54,55]. We did, however, find hypersusceptibility in zebrafish using cyclosporin A, another Ppp3/calcein inhibitor associated with clinical IA.

In the absence of effective adaptive immunity, innate immune phagocytes shape the pathophysiology of infections caused by the more than 300 fungal species pathogenic to humans, including *A. fumigatus* [56]. To devise HDTs effective against IA, we looked at the possible intracellular degradation pathways in innate immune phagocytes for conidia during the first stages of infection by analyzing GFP-Lc3 interaction with conidia. Autophagy pathways have been previously reported to be affected during immunosuppressive treatment against IA and in chronic granulomatous disease patients [52,57], and the autophagy-related pathway LAP has been linked to efficient fungal clearance of *A. fumigatus* conidia by macrophages [22,23,58,59]. During LAP, conidia are transported into single-membrane vesicles, which undergo a Reactive Oxygen Species (ROS) production burst and become decorated with LC3 for rapid degradation [58]. However, the DHN-melanin coating of *A. fumigatus* conidia inhibits the ROS production required for the processing of intracellular vesicles and its ultimate fusing with lysosomes [24,25,45]. This antagonism results in a dynamic interaction between the host and the pathogen. Indeed, in infections with

f) Survival curves of *atg13* mutation (e) or *rubcn* (f) knockdown or control zebrafish embryos infected with *A. fumigatus* Δ *pksP*. (G, H, I, J, and K) Quantification of phagocytosis and Lc3 dynamics in 21 hours of timelapse imaging from 5 individual larvae infected with *A. fumigatus* Δ *pksP* conidia labeled with Alexa Fluor™ NHS 647 during the first hours post infection. (g) Most of the injected conidia in the zebrafish hindbrain are phagocytosed by macrophages, and (h) macrophages phagocytose more conidia per cell than neutrophils. (i, j, and k) In the events of conidial phagocytosis by neutrophils, we observed rapid bright Lc3 rings covering single-conidia vesicles, while Lc3 decoration of conidia-containing vesicles in macrophages was scarcer and shorter in the first hours post infection. Examples of GFP-Lc3 signal around single *A. fumigatus* Δ *pksP* conidia labeled with Alexa Fluor™ NHS 647 (Af Δ *pksP*) in mCherryF negative phagocytes (l, m), or mCherryF labeled macrophage (n). Images taken from Movie S4. All survival curves are representative of at least 3 independent biological replicates. The hazard ratio (HR) indicated is calculated vs. the control condition using the logrank method. Significance in the curve comparison is calculated using Log-rank (Mantel-Cox test): ns non-significant; * $P \leq 0.05$; ** $P \leq 0.01$; *** $P \leq 0.001$; **** $P \leq 0.0001$.

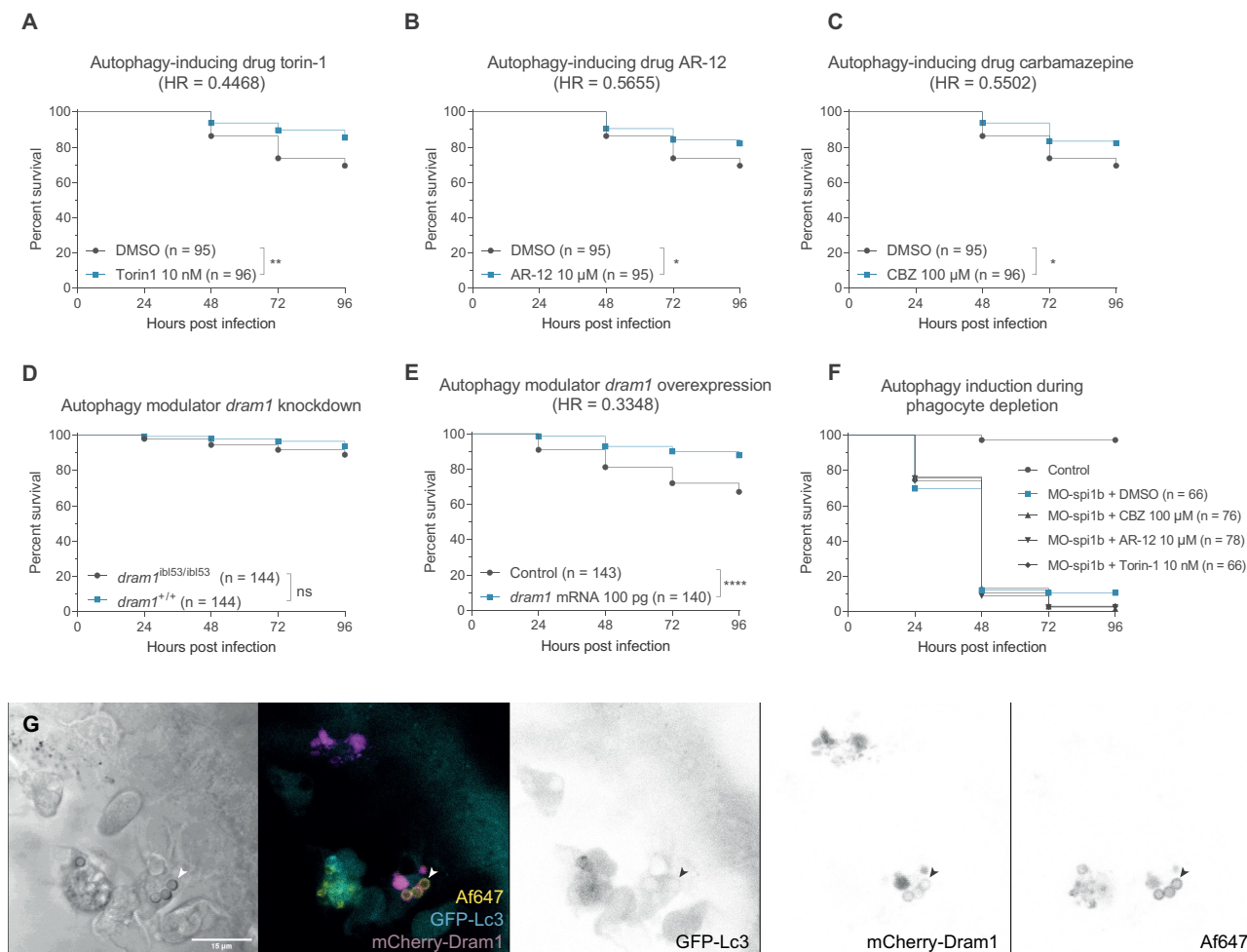


Figure 5. Stimulating the (auto)phagolysosomal axis increases the host survival against IA. (a, b and c) Survival curves of zebrafish embryos infected with *A. fumigatus* $\Delta Ku80$ and exposed via waterborne treatment to 10 nM of torin 1 (a), 10 μ M of AR-12 (b), 100 μ M or carbamazepine (c), or DMSO as a vehicle control at the same v.v. (a, b, and c) infections were performed together but showed in split graphs for visualization purposes. (d) Survival curve of *dram1* mutants or non-mutant siblings infected with *A. fumigatus* $\Delta Ku80$. (e) Survival curve of zebrafish embryos overexpressing *Dram1* after injection of 100 pg of *dram1* mRNA or their control infected with *A. fumigatus* $\Delta Ku80$. (f) Confocal image demonstrating colocalization (arrowheads) of mCherry-Dram1 with Alexa Fluor™ NHS 647-labeled *A. fumigatus* conidia (Af647) inside a phagocyte in the zebrafish hindbrain shortly after infection. All survival curves are representative of at least 3 independent biological replicates. The hazard ratio (HR) indicated is calculated vs. the control condition using the logrank method. Significance in the curve comparison is calculated using Log-rank (Mantel-Cox test): ns non-significant; * $P \leq 0.05$; ** $P \leq 0.01$; *** $P \leq 0.001$; **** $P \leq 0.0001$.

both wild type and DHN-melanin-deficient conidia, we observed GFP-Lc3 association with single and multiple conidia-containing vesicles that persisted from the first stages after phagocytosis to the initial stages of fungal germination.

Despite efficiently phagocytosing *A. fumigatus* conidia, macrophages are unable to efficiently kill them, and it has been suggested that they may provide a safe compartment from which *A. fumigatus* can eventually germinate [28]. Contrasting, neutrophils can kill *A. fumigatus* conidia via PI3K-dependent nonoxidative pathways (i.e., via Fe^{2+} sequestration) [60]. However, it has been reported that neutrophils are usually not engaged during the first stages of *A. fumigatus* infection, but mostly after fungal germination, where ROS production (e.g., via *cyba*) is crucial to contain dimorphic fungal growth [17,33]. Here, we uncovered an additional piece of information regarding the differences between macrophages and neutrophils in dealing with intracellular *A. fumigatus* conidia: in the rare event of conidial phagocytosis by neutrophils, we observed a rapid and bright GFP-Lc3

targeting to vesicles containing single conidia, contrasting with the weaker mobilization of GFP-Lc3 in macrophages. It is important to mention that in these analyses we probably underestimated the colocalization events and their duration due to the speed at which they happen intracellularly, fluorescent reporter levels, and cells moving outside of the imaging focus after phagocytosing conidia. It has also been recently reported how inhibition of *tyr/Tyr* (Tyrosinase) function (e.g., via the use of N-phenylthiourea [PTU], which we used during intravital imaging) increases the autophagy flux in zebrafish embryos 24 h after treatment [61], which may also affect the quantification levels shown in this study.

In addition, while neutrophils phagocytosed less conidia than macrophages per cell, we did not see a similar GFP-Lc3 activation in macrophages with a similar low amount of phagocytosed conidia. It has been established that macrophages can mount host-protective xenophagy and LAP responses against *Mycobacteria* and *Salmonella* [44,62]. Therefore, the differences that we observe are, at least

partially, related to the interaction of these immune cells with the fungal conidia, and not to their intrinsic capability of activating autophagy-related processes. In concordance, we hypothesized that the autophagic defenses in macrophages are inhibited during *A. fumigatus* infection in a DHN-melanin-dependent manner and that pharmacological activation of these defense mechanisms may improve the clinical outcome of IA. Given the previously discussed role of DHN-melanin in inhibiting autophagy-related processes via calcium sequestration, neutrophils may use different nonoxidative or calcium-independent oxidative ROS production pathways to stabilize LC3 in the phagosomal membrane. Therefore, a potential HDT avenue to provide better host defense against *A. fumigatus* lies in incrementing the function or number of neutrophils, or the leukocyte ratio of neutrophils to macrophages, as others have highlighted [39].

Consistent with the multiple autophagy-related processes that we observed in the host-pathogen interaction, we demonstrated by loss-of-function experiments that not only LAP, but also Atg13-mediated and Sqstm1-independent autophagy processes are relevant for the overall host survival during *A. fumigatus* infection. Therefore, despite that *A. fumigatus* conidia may be initially captured intracellularly via LAP, additional antimicrobial autophagy processes are relevant to the antifungal host defense in the course of the infection. Having confirmed the requirement of (auto)phagolysosomal pathways in host defense against IA *in vivo*, we demonstrated that their stimulation provides a host-dependent protective effect to the fungal infection. To do so, we used pharmacological and genetic methods to induce these processes via independent pathways, both MTOR dependent and independent. It has recently been published how the DHN-melanin from *A. fumigatus* conidia can affect macrophage metabolism via CALM (calmodulin) and MTOR and may therefore be a potential interesting target to design therapies against IA [46,63]. Based on the results that we report here, we now expand on the potential HDT targets in metabolism to include other (auto)phagolysosomal pathways, inducible by the autophagy modulator DRAM1 and drugs including AR-12, torin-1 and carbamazepine. However, it is important that the stimulation of these pathways does not create secondary immunosuppressant effects, such as in rapamycin treatment, which is known as a classical macroautophagy inducer via MTOR modulation, but also results in higher mortality to the infection.

In this work, we used the zebrafish embryo model to study the effect of hindering and inducing autophagy activation against *A. fumigatus* infection. Autophagy is involved in a wide range of physiological responses and maintaining homeostasis in addition to its impact on host immunity. In that sense, completely blocking autophagy during long periods of time (e.g., pharmacologically via bafilomycin) or permanently knocking-out of one of its core proteins, such as Atg5, is lethal for a developing zebrafish larva, as it is for mice [64]. Therefore, in this study we opted for abolishing specific initiation processes (selective autophagy via *atg13* and LAP via *rubcn*) and autophagy receptors (*sqstm1*), which may be compensated for via other mechanisms. In a similar way, all the activation treatments were performed in a whole-

organism level. To discard a possible effect of the treatments in increasing tolerance to the infection or directly to *A. fumigatus*, we showed that these treatments do not increase survival in the absence of phagocytes, demonstrated colocalization of mCherry-Dram1 with phagocytosed conidia, and that they do not affect the growth and germination of *A. fumigatus in vitro*, thus confirming that the treatments work by modulating the immune response to the infection.

Despite that we only focused on visualizing the intracellular effects against *A. fumigatus* conidia shortly after phagocytosis, the stimulation of the (auto)phagolysosomal pathways may boost the antifungal host defense at several stages of the infection process. That is, on top of stimulating the fusion of *Aspergillus*-containing phagosomes (either captured via LAP or xenophagy) with lysosomes, autophagic processes may also be involved in the production of antimicrobial peptides [65], stimulating ROS and neutrophil extracellular trap/NET production against hyphae [66], the lateral transfer of conidia between overburdened macrophages [53], or hypothetically even containing the infection spread via entosis-related pathways. Furthermore, the stimulation of these pathways may synergize with current treatments by providing increased intracellular conidial constriction, thus allowing more exposure to antifungals in infected cells [67]. It would therefore be interesting to explore how different autophagy processes contribute to these processes and their relevance against IA.

Finally, the autophagy machinery has already been suggested as a target for HDT design against several infections [11,13]. For example, autophagy processes are crucial in the defense against mycobacteria [68], and have been proposed as potential HDTs to fight drug-resistant tuberculosis [69], one of the most common IA comorbidities. Therefore, stimulating the (auto)phagolysosomal pathways may be of special interest in specific cases where it may provide synergistic benefits against combined infections.

In all, we visualized autophagy responses *in vivo* shortly after conidial phagocytosis and demonstrated how they are relevant to the host survival in response to IA in a population perspective using an immunocompromised animal model. In doing so, we highlight that (auto)phagolysosomal pathways are an interesting target to develop HDTs against this fungal infection and should be explored for their potential use in settings with prevalence of drug-resistant *Aspergillus* infections.

Materials and methods

Zebrafish husbandry

Zebrafish were handled in compliance with the local animal welfare directives of Leiden University (License number 10,612) and following standard zebrafish rearing protocols (<https://zfin.org>), which adhere to the international guidelines from the EU Animal Protection Direction 2010/63/EU. In this work we used the lines ABTL (wild-type), Tg(CMV:EGFP-*map1lc3b*)^{zfl155}, Tg(*bactin*:mCherry-*map1lc3b*) [38], Tg(CMV:EGFP-*map1lc3b*)^{zfl155}; *mpeg1.1*:mCherry^{F^{ump2}}, Tg(*mpeg1.1*:EGFP)^{sl22}, *mpx*:GAL4-VP16^{sh267}/UAS-E1B:NTR-mCherry¹¹⁴⁹, and Tg(*mpx*:GAL4-VP16^{sh267}/UAS-E1B:NTR-mCherry¹¹⁴⁹). All experiments were performed on zebrafish

embryos or larvae up to 5 days post fertilization, which have not yet reached the free-feeding stage. Embryos were collected in egg water (Sera Marin salt, 05420; 60 µg/ml in distilled deionized water) and maintained in E3-buffered medium (300 mM NaCl, 10.2 mM KCl, 19.8 mM CaCl₂ · 2 H₂O, 19.8 mM MgSO₄ · 7H₂O in egg water) at 28.5°C for the duration of the experiments. Prior to infections, imaging and fixation, embryos were anaesthetized with 0.02% buffered 3-aminobenzoic acid ethyl ester (tricaine; Sigma-Aldrich, A-5040).

Fungal culture

Fungal strains used in this study (*A. fumigatus* Δ*Ku80* as wild-type, Δ*pksP*, D141 with *PgpdA::dsRed* in pAN7.1 [40], and D141 with *PgpdA::EGFP* in pAN7.1) were inoculated onto fresh plates of Complete Medium, containing 1% (w:v) glucose (VWR, 24,379.363), 7 mM KCl (VWR, 26,759.291), 11 mM KH₂PO₄ (VWR, 26,925.295), pH 6.8, 70 mM NaNO₃ (VWR, 27,950.298), 2 mM MgSO₄ (VWR, 25,163.290), 76 nM ZnSO₄ (Sigma-Aldrich, Z0251), 178 nM H₃BO₃ (VWR, 20,181.294), 25 nM MnCl₂ (Sigma-Aldrich, M3634), 18 nM FeSO₄ (Sigma-Aldrich, F8633), 7.1 nM CoCl₂ (Sigma-Aldrich, C8661), 6.4 nM CuSO₄ (Sigma-Aldrich, C8027), 6.2 nM Na₂MoO₄ (Sigma-Aldrich, S6646), 174 nM EDTA (VWR, 20,296.291), 0.5% (w:v) yeast extract (VWR, 84,601.5000) and 0.1% (w:v) casamino acids (BD Biosciences, 223,050) for 72 h at 37°C. Spores were then harvested in Phosphate Saline Buffer and filtered through 2 layers of Miracloth and adjusted to a concentration of 1.5 × 10⁸ spores/ml as measured by automated cell counter (Bio-Rad TC20). If required, spores were labeled with Alexa Fluor™ 647 NHS Ester (Thermo Fisher, A20006) following manufacturer's protocol. Spore batches were kept at 4°C for a maximum of 4 weeks and resuspended in 5% (w:v) polyvinylpyrrolidone (PVP40, Sigma-Aldrich, 9003–39-8) in phosphate-buffered saline (PBS; Thermo Scientific, 28,908) at a concentration of 1.0 × 10⁸ conidia/ml prior to injection.

The analysis of the direct drug effect on *A. fumigatus* growth was adapted from previously described [70]. Briefly, 100 µl of Minimum Media with 0.006% yeast extract (w:v) were combined with 100 µl at 2, 4, or 8 × 10⁵ conidia/ml in a white, clear-bottomed, 96-well plate (Greiner Bio-one, 655,095). Subsequently, 20 µl of the drugs or DMSO as vehicle control were added to each well to the final concentration used in zebrafish experiments. Plates were incubated at 30°C with continuous measuring of OD₆₀₀ in a EnSpire Multiplate Reader (Perkin Elmer).

Morpholino, RNA and cas9 injections

Previously validated *atg13* (1 mM) [44], *cyba* (1 mM) [33], *rbcn* (0.25 mM) [44], and *spi1b* (1 mM) [49] morpholinos (Gene Tools) were resuspended in Milli-Q water and diluted in Danieau Buffer (58 mM NaCl, 0.7 mM KCl, 0.4 mM MgSO₄, 0.6 mM Ca(NO₃)₂, 5.0 mM HEPES, pH 7.6). The polyadenylated *Dram1* mRNA and mCherry-*Dram1* constructs were synthesized and concentrated as previously described [47]. To generate F0 crispants, three independent

predesigned crRNA guides targeting *atg13* (Integrated DNA Technologies Europe, ATG13.1.AA, ATG13.1.AB, and ATG13.1.AD), *cyba* (Integrated DNA Technologies Europe, CYBA.1.AA, CYBA.1.AB, and CYBA.1.AC), and negative control *scrambl* crRNA (Integrated DNA Technologies Europe, Negative Control crRNA #1, #2, and #3) were processed as previously described [34]. Briefly, the crRNAs were annealed with tracrRNA (Integrated DNA Technologies Europe) to generate gRNA, which were assembled with Alt-R S.p. Cas9 Nuclease V3 (Integrated DNA Technologies Europe, 1,081,063) to generate RNPs. The three RNPs for each gene were then pooled prior to injection at a final concentration of 30.5 µM per gene (10.1 µM per independent RNP). In addition, *tyr*-targeting crRNAs (Integrated DNA Technologies Europe, TYR.1.AA, TYR.1.AB, and TYR.1.AC) were used in each batch to confirm Cas9 activity. One-cell stage zebrafish embryos were microinjected with 1nL of the morpholino, RNA, or Cas9 solution in the yolk.

The *rbcn* knockdown after morpholino injection was corroborated by PCR and gel electrophoresis using the primers specified in Table S1, while the lack of immune cells after MO-*spi1b* injection was corroborated by stereo fluorescence imaging in the Tg(*mpeg1.1:EGFP*^{gl22}, *mpx:GAL4-VP16*^{sh267}/UAS-E1B:NTR-mCherry¹⁴⁹) strain. The effectivity of the mutation of the *atg13* and *cyba* guides was corroborated in each batch by extracting DNA according to a modified HOTSHOT DNA extraction protocol [34], followed by qPCR amplification with Power SYBR Green Master Mix (Applied Biosystems, A25742) following manufacturer's protocol and melt curve analysis for each targeted locus. The primers used for each locus are specified in Table S1.

Fungal infections

Embryos were manually dechorionated using jeweler forceps prior to infection. Approximately 100 conidia (as visually verified during the injections at 120X magnification) were injected into the zebrafish hindbrain ventricle via the otic vesicle at 30–32 hpf as previously described [40]. After infection, embryos were inspected for possible damage during manipulation and, in the case of drug treatments, randomly distributed in different groups for survival analysis. For survival assays, embryos were individually distributed in 48-well plates containing 500 µl of drug-containing E3 medium and monitored every 24 h up to 5 days post fertilization.

Drug treatments

Dexamethasone (Sigma-Aldrich, D1756-25 MG), FK506 (InvivoGen, tlr1-fk5), rapamycin (Sigma-Aldrich, 44,532-U), cyclosporin A, metronidazole (Sigma-Aldrich, M1547-5 G), AR-12 (MedChem Express, HY-10547_5 mg), carbamazepine (MedChem Express, HY-B0246-100 mg), torin 1 (MedChem Express, HY-13003_5 mg), and voriconazole (Sigma-Aldrich, PZ0005-5 MG) were resuspended at 10 mg/ml in DMSO (Sigma-Aldrich, 154,938) and aliquoted in 100 µl stock concentrations at the recommended temperature for long-term storage for each drug. Working aliquots were kept at 4°C for

a maximum of 4 weeks and added to the E3 water at the final concentration stated immediately after zebrafish inspection and before being transferred to individual wells.

Statistical analysis

All survival experiments were performed at least in triplicate and pooled into a final number of individuals stated using the Kaplan-Meier method. Pairwise comparisons of survival curves were performed using the Log-rank (Mantel-Cox) test in GraphPad Prism version 8.0. Statistical significance was assumed at p-value below 0.05. For each survival experiment, the hazard ratio via the logrank method is also reported.

Confocal microscopy

For microscopy experiments, 0.2 mM PTU (Sigma-Aldrich, P7629) was added to the E3 medium at 24 hpf to prevent pigmentation. For non-live confocal microscopy (Figures 2(h, I)), embryos were fixed at 15 h post infection using a 4% formaldehyde solution in PBS overnight, and then stored in PBS for up to 3 days before imaging. For live imaging, live infected embryos were mounted in 2% low melting agarose (SERVA, 140,727) in E3 medium containing 0.2 mM PTU and 0.02% tricaine. The hindbrain ventricle region was imaged using a Leica TCS SP8 confocal microscope with a 40X or 63X oil immersion objective (NA = 1.4), equipped with 488-nm, 532-nm, and 638-nm laser lines.

Abbreviation list

DMSO: dimethyl sulfoxide; HR: hazard ratio; HDT: host-directed therapy; Hpf: hours post fertilization; IA: invasive Aspergillosis; LAP: LC3-associated phagocytosis; MTZ: metronidazole; PTU: N-phenylthiourea; ROS: reactive oxygen species.

Acknowledgments

We thank Michiel van der Vaart and Monica Varela for confocal microscopy advice and critical proofreading of the manuscript, and all members of the fish facility team for zebrafish care at the Institute of Biology Leiden. The *A. fumigatus* melanin-deficient strain $\Delta pksP$ was a kind gift from Dr. Jean-Paul Latgé (Institut Pasteur, Paris, France). The fluorescent zebrafish lines labelling Lc3, macrophages or neutrophils were kind gifts from Dan Klionsky (University of Michigan, USA), Georges Lutfalla (University of Montpellier, France), and Stephen Renshaw (University of Sheffield). This work and G.F.-C. were supported by a European Marie Curie fellowship (H2020-COFUND-2015-FP707404).

Disclosure statement

No potential conflict of interest was reported by the author(s).

Funding

This work was supported by the H2020 Marie Skłodowska-Curie Actions [H2020-COFUND-2015-FP707404].

Data availability statement

All images presented in this manuscript except Figure 2D-I, and 5F are stills from confocal timelapse imaging experiments. All raw confocal imaging data is freely available for download and reuse via Biostudies under accession number S-BSST698 (<https://www.ebi.ac.uk/biostudies/studies/S-BSST698>), in which each file is tagged with the figures that belong to it.

ORCID

G Forn-Cuní  <http://orcid.org/0000-0001-5976-4759>
L Welvaarts  <http://orcid.org/0000-0002-2160-5186>
FM Stel  <http://orcid.org/0000-0002-3781-8223>
CJ van den Hondel  <http://orcid.org/0000-0003-4782-2725>
M Arentshorst  <http://orcid.org/0000-0001-7693-9370>
AFJ Ram  <http://orcid.org/0000-0002-2487-8016>
AH Meijer  <http://orcid.org/0000-0002-1325-0725>

References

- [1] Aimanianda V, Bayry J, Bozza S, et al. Surface hydrophobin prevents immune recognition of airborne fungal spores. *Nature*. 2009;460:1117–1121.
- [2] Stop neglecting fungi. *Nat Microbiol*. 2017;2:17120.
- [3] Kousha M, Tadi R, Soubani AO. Pulmonary aspergillosis: a clinical review. *Eur Respir Rev Off J Eur Respir Soc*. 2011;20:156–174.
- [4] Burgos A, Zaoutis TE, Dvorak CC, et al. Pediatric invasive aspergillosis: a multicenter retrospective analysis of 139 contemporary cases. *Pediatrics*. 2008;121:e1286–1294.
- [5] van Paassen J, Russcher A, and In 't Veld-van Wingerden AW, et al. Emerging aspergillosis by azole-resistant *Aspergillus fumigatus* at an intensive care unit in the Netherlands, 2010 to 2013. *Euro Surveill Bull Eur Sur Mal Transm Eur Commun Dis Bull*. 2016;21(30):30300. <https://www.nature.com/articles/nmicrobiol2017120>
- [6] Berger S, El Chazli Y, Babu AF, et al. Azole resistance in aspergillus fumigatus: a consequence of antifungal use in agriculture? *Front Microbiol*. 2017;8:1024.
- [7] Pappas PG, Alexander BD, Andes DR, et al. Invasive fungal infections among organ transplant recipients: results of the transplant-associated infection surveillance network (TRANSNET). *Clin Infect Dis Off Publ Infect Dis Soc Am*. 2010;50:1101–1111.
- [8] Kosmidis C, Denning DW. The clinical spectrum of pulmonary aspergillosis. *Thorax*. 2015;70:270–277.
- [9] Schauwvlieghe AFAD, Rijnders BJA, Philips N, et al. Invasive aspergillosis in patients admitted to the intensive care unit with severe influenza: a retrospective cohort study. *Lancet Respir Med*. 2018;6:782–792.
- [10] Barac A, Kosmidis C, Alastruey-Izquierdo A, et al. Chronic pulmonary aspergillosis update: a year in review. *Med Mycol*. 2019;57:S104–S109.
- [11] Armstrong-James D, Brown GD, Netea MG, et al. Immunotherapeutic approaches to treatment of fungal diseases. *Lancet Infect Dis*. 2017;17:e393–e402.
- [12] Kaufmann SHE, Dorhoi A, Hotchkiss RS, et al. Host-directed therapies for bacterial and viral infections. *Nat Rev Drug Discov*. 2018;17:35–56.
- [13] Karavalakis G, Yannaki E, Papadopoulou A. Reinforcing the immunocompromised host defense against fungi: progress beyond the current state of the art. *J Fungi Basel Switz*. 2021;7:451.
- [14] Oikonomou V, Renga G, De Luca A, et al. Autophagy and LAP in the fight against fungal infections: regulation and therapeutics. *Mediators Inflamm*. 2018;2018:6195958.
- [15] Deretic V, Saitoh T, Akira S. Autophagy in infection, inflammation and immunity. *Nat Rev Immunol*. 2013;13:722–737.

- [16] Maiuri MC, Kroemer G. Therapeutic modulation of autophagy: which disease comes first? *Cell Death Differ.* **2019**;26:680–689.
- [17] van de Veerdonk FL, Gresnigt MS, Romani L, et al. *Aspergillus fumigatus* morphology and dynamic host interactions. *Nat Rev Microbiol.* **2017**;15:661–674.
- [18] Segal BH. Role of macrophages in host defense against aspergillosis and strategies for immune augmentation. *Oncologist.* **2007**;12 Suppl 2:7–13.
- [19] Margalit A, Kavanagh K. The innate immune response to *Aspergillus fumigatus* at the alveolar surface. *FEMS Microbiol Rev.* **2015**;39:670–687.
- [20] Ibrahim-Granet O, Philippe B, Boleti H, et al. Phagocytosis and intracellular fate of *Aspergillus fumigatus* conidia in alveolar macrophages. *Infect Immun.* **2003**;71:891–903.
- [21] Seidel C, Moreno-Velásquez SD, Ben-Ghazzi N, et al. Phagolysosomal survival enables non-lytic hyphal escape and ramification through lung epithelium during *aspergillus fumigatus* infection. *Front Microbiol.* **2020**;11:1955.
- [22] Martinez J, Malireddi RKS, Lu Q, et al. Molecular characterization of LC3-associated phagocytosis reveals distinct roles for Rubicon, NOX2 and autophagy proteins. *Nat Cell Biol.* **2015**;17:893–906.
- [23] Sprenkeler EGG, Gresnigt MS, van de Veerdonk FL. LC3-associated phagocytosis: a crucial mechanism for antifungal host defence against *Aspergillus fumigatus*. *Cell Microbiol.* **2016**;18:1208–1216.
- [24] Chamilos G, Akoumianaki T, Kyrmizi I, et al. Melanin targets LC3-associated phagocytosis (LAP): a novel pathogenetic mechanism in fungal disease. *Autophagy.* **2016**;12:888–889.
- [25] Kyrmizi I, Ferreira H, Carvalho A, et al. Calcium sequestration by fungal melanin inhibits calcium-calmodulin signalling to prevent LC3-associated phagocytosis. *Nat Microbiol.* **2018**;3:791–803.
- [26] Knox BP, Deng Q, Rood M, et al. Distinct innate immune phagocyte responses to *Aspergillus fumigatus* conidia and hyphae in zebrafish larvae. *Eukaryot Cell.* **2014**;13:1266–1277.
- [27] Rosowski EE, Knox BP, Archambault LS, et al. The zebrafish as a model host for invasive fungal infections. *J Fungi Basel Switz.* **2018**;4:E136.
- [28] Rosowski EE, Raffa N, Knox BP, et al. Macrophages inhibit *Aspergillus fumigatus* germination and neutrophil-mediated fungal killing. *PLoS Pathog.* **2018**;14:e1007229.
- [29] Herbst S, Shah A, Mazon Moya M, et al. Phagocytosis-dependent activation of a TLR9-BTK-calcineurin-NFAT pathway co-ordinates innate immunity to *Aspergillus fumigatus*. *EMBO Mol Med.* **2015**;7:240–258.
- [30] Trede NS, Langenau DM, Traver D, et al. The use of zebrafish to understand immunity. *Immunity.* **2004**;20:367–379.
- [31] Santoriello C, Zon LI. Hooked! Modeling human disease in zebrafish. *J Clin Invest.* **2012**;122:2337–2343.
- [32] Muñoz-Sánchez S, van der Vaart M, Meijer AH. Autophagy and Lc3-associated phagocytosis in zebrafish models of bacterial infections. *Cells.* **2020**;9:E2372.
- [33] Schoen TJ, Rosowski EE, Knox BP, et al. Neutrophil phagocyte oxidase activity controls invasive fungal growth and inflammation in zebrafish. *J Cell Sci.* **2019**;133:jcs236539.
- [34] Kroll F, Powell GT, Ghosh M, et al. A simple and effective F0 knockout method for rapid screening of behaviour and other complex phenotypes. *eLife.* **2021**;10:e59683.
- [35] Curado S, Stainier DYR, Anderson RM. Nitroreductase-mediated cell/tissue ablation in zebrafish: a spatially and temporally controlled ablation method with applications in developmental and regeneration studies. *Nat Protoc.* **2008**;3:948–954.
- [36] Knox BP, Huttenlocher A, Keller NP. Real-time visualization of immune cell clearance of *Aspergillus fumigatus* spores and hyphae. *Fungal Genet Biol FG B.* **2017**;105:52–54.
- [37] He C, Bartholomew CR, Zhou W, et al. Assaying autophagic activity in transgenic GFP-Lc3 and GFP-Gabarap zebrafish embryos. *Autophagy.* **2009**;5:520–526.
- [38] van der Vaart M, Banducci-Karp A, Forn-Cuní G, et al. DRAM1 requires PI(3,5)P2 generation by PIKfyve to deliver vesicles and their cargo to endolysosomes. *bioRxiv.* **2020**; Internet cited 2022 May 16:2020.12.15.422832. Available from <https://www.biorxiv.org/content/10.1101/2020.12.15.422832v2>
- [39] Ellett F, Pazhakh V, Pase L, et al. Macrophages protect *Talaromyces marneffi* conidia from myeloperoxidase-dependent neutrophil fungicidal activity during infection establishment in vivo. *PLoS Pathog.* **2018**;14:e1007063.
- [40] Koch BEV, Hajdamowicz NH, Lagendijk E, et al. *Aspergillus fumigatus* establishes infection in zebrafish by germination of phagocytized conidia, while *Aspergillus niger* relies on extracellular germination. *Sci Rep.* **2019**;9:12791.
- [41] Bonnett CR, Cornish EJ, Harmsen AG, et al. Early neutrophil recruitment and aggregation in the murine lung inhibit germination of *aspergillus fumigatus* conidia. *Infect Immun.* **2006**;74:6528–6539.
- [42] Masud S, Torraca V, Meijer AH. Modeling infectious diseases in the context of a developing immune system. *Curr Top Dev Biol.* **2017**;124:277–329.
- [43] Masud S, van der Burg L, Storm L, et al. Rubicon-dependent Lc3 recruitment to salmonella-containing phagosomes is a host defense mechanism triggered independently from major bacterial virulence factors. *Front Cell Infect Microbiol.* **2019**;9:279.
- [44] Masud S, Prajsnar TK, Torraca V, et al. Macrophages target salmonella by Lc3-associated phagocytosis in a systemic infection model. *Autophagy.* **2019**;15:796–812.
- [45] Akoumianaki T, Kyrmizi I, Valsecchi I, et al. *Aspergillus* cell wall melanin blocks LC3-Associated phagocytosis to promote pathogenicity. *Cell Host Microbe.* **2016**;19:79–90.
- [46] Gonçalves SM, Duarte-Oliveira C, Campos CF, et al. Phagosomal removal of fungal melanin reprograms macrophage metabolism to promote antifungal immunity. *Nat Commun.* **2020**;11:2282.
- [47] van der Vaart M, Korbee CJ, Lamers GEM, et al. The DNA damage-regulated autophagy modulator DRAM1 links mycobacterial recognition via TLR-MYD88 to autophagic defense [corrected]. *Cell Host Microbe.* **2014**;15:753–767.
- [48] Masud S, Zhang R, Prajsnar TK, et al. Dram1 confers resistance to Salmonella infection. *bioRxiv.* **2021** Mar 21;436194 .
- [49] Bukrinsky A, Griffin KJP, Zhao Y, et al. Essential role of spi-1-like (spi-1l) in zebrafish myeloid cell differentiation. *Blood.* **2009**;113:2038–2046.
- [50] Centers for Disease Control and Prevention (U.S.). Antibiotic resistance threats in the United States, 2019 [Internet]. Centers for Disease Control and Prevention (U.S.); cited 2021 Jun 29]. Available from: <https://stacks.cdc.gov/view/cdc/82532>.
- [51] Fisher MC, Hawkins NJ, Sanglard D, et al. Worldwide emergence of resistance to antifungal drugs challenges human health and food security. *Science.* **2018**;360:739–742.
- [52] Kyrmizi I, Gresnigt MS, Akoumianaki T, et al. Corticosteroids block autophagy protein recruitment in *aspergillus fumigatus* phagosomes via targeting dectin-1/Syk kinase signaling. *J Immunol.* **2013**;191:1287–1299.
- [53] Shah A, Kannambath S, Herbst S, et al. Calcineurin orchestrates lateral transfer of *Aspergillus fumigatus* during macrophage cell death. *Am J Respir Crit Care Med.* **2016**;194:1127–1139.
- [54] Knox BP, Blachowicz A, Palmer JM, et al. Characterization of *Aspergillus fumigatus* isolates from air and surfaces of the international space station. *mSphere.* **2016**;1:e00227–16.
- [55] Keizer EM, Valdes ID, Forn-Cuní G, et al. Variation of virulence of five *Aspergillus fumigatus* isolates in four different infection models. *PLoS One.* **2021**;16:e0252948.
- [56] Hünninger K, Kurzai O. Phagocytes as central players in the defence against invasive fungal infection. *Semin Cell Dev Biol.* **2019**;89:3–15.
- [57] de Luca A, Smeekens SP, Casagrande A, et al. IL-1 receptor blockade restores autophagy and reduces inflammation in chronic

- granulomatous disease in mice and in humans. *Proc Natl Acad Sci U S A*. 2014;111:3526–3531.
- [58] Herb M, Gluschko A, Schramm M. LC3-associated phagocytosis - The highway to hell for phagocytosed microbes. *Semin Cell Dev Biol*. 2020;101:68–76.
- [59] Akoumianaki T, Vaporidi K, and Diamantaki E, et al. Uncoupling of IL-6 signaling and LC3-associated phagocytosis drives immunoparalysis during sepsis. *Cell Host Microbe*. 2021;29(8):1277–1293.e6.
- [60] Gazendam RP, van Hamme JL, Tool ATJ, et al. Human neutrophils use different mechanisms to kill *Aspergillus fumigatus* conidia and hyphae: evidence from phagocyte defects. *J Immunol Baltim Md*. 2016;196:1272–1283. 1950
- [61] Chen X-K, Kwan JS-K, Chang R-C-C, et al. 1-phenyl 2-thiourea (PTU) activates autophagy in zebrafish embryos. *Autophagy*. 2021;17:1222–1231.
- [62] Zhang R, Varela M, Vallentgoed W, et al. The selective autophagy receptors optineurin and p62 are both required for zebrafish host resistance to mycobacterial infection. *PLoS Pathog*. 2019;15:e1007329.
- [63] Papon N, Gangneux J-P, Delneste Y. Fungal Melanin Rewires Macrophage Metabolism. *Trends Biochem Sci*. 2020;45:728–730.
- [64] Mans LA, Querol Cano L, van Pelt J, et al. The tumor suppressor LKB1 regulates starvation-induced autophagy under systemic metabolic stress. *Sci Rep*. 2017;7:7327.
- [65] Gomes LC, Dikic I. Autophagy in antimicrobial immunity. *Mol Cell*. 2014;54:224–233.
- [66] Skendros P, Mitroulis I, Ritis K. Autophagy in neutrophils: from granulopoiesis to neutrophil extracellular traps. *Front Cell Dev Biol*. 2018;6:109.
- [67] Rosowski EE, He J, Huisken J, et al. Efficacy of voriconazole against *Aspergillus fumigatus* infection depends on host immune function. *Antimicrob Agents Chemother*. 2020;64:e00917–19.
- [68] Gutierrez MG, Master SS, Singh SB, et al. Autophagy is a defense mechanism inhibiting BCG and mycobacterium tuberculosis survival in infected macrophages. *Cell*. 2004;119:753–766.
- [69] Kilinç G, Saris A, Ottenhoff THM, et al. Host-directed therapy to combat mycobacterial infections. *Immunol Rev*. 2021;301:62–83.
- [70] Rocha MC, Fabri JHTM, Franco de Godoy K, et al. *Aspergillus fumigatus* MADS-box transcription factor *rlma* is required for regulation of the cell wall integrity and virulence. *G3 Bethesda Md*. 2016;6:2983–3002.